Helical Quantum States in HgTe Quantum Dots with Inverted Band Structures

Kai Chang and Wen-Kai Lou

SKLSM, Institute of Semiconductors, Chinese Academy of Sciences, P.O. Box 912, Beijing 100083, China
Beijing Computational Science Research Center, Beijing, 100089, China

(Received 6 October 2010; published 16 May 2011)

We investigate theoretically the electron states in HgTe quantum dots (QDs) with inverted band structures. In sharp contrast to conventional semiconductor quantum dots, the quantum states in the gap of the HgTe QD are fully spin-polarized and show ringlike density distributions near the boundary of the QD and spin-angular momentum locking. The persistent charge currents and magnetic moments, i.e., the Aharonov-Bohm effect, can be observed in such a QD structure. This feature offers us a practical way to detect these exotic ringlike edge states by using the SQUID technique.

DOI: 10.1103/PhysRevLett.106.206802 PACS numbers: 73.21.La, 71.70.Di, 71.70.Ej, 73.23.Ra

Semiconductor quantum dots (QDs) have attracted intensive attention in the past decades due to their application in electronic devices [1,2], e.g., single-electron transistors [3], light-emitting diodes [4], diode lasers [5], and solar cells [6]. The electron and hole ground states both localize at the central part of the QDs, which gives rise to a strong oscillator strength of the interband optical transition. This is the common feature for various semiconductor QDs with a positive band gap, e.g., self-assembled InAs [7] and GaAs quantum dots [8,9]. Precise control of quantum states in QDs pave the way to realize highly desirable key functions in nanoelectronics, quantum computing, and quantum information processing.

By decreasing the band gap, the band structure can be inverted [10]. In this case, HgTe becomes insulating in the bulk with a gap separating the valence and conduction bands but with gapless helical edge states that are topologically protected by the time-reversal symmetry, named a topological insulator (TI) [11,12]. This topological insulator, one of the recent remarkable discoveries, is a new state of quantum matter [11,13–16]. The quantum spin Hall effect in such two-dimensional TIs was predicted theoretically [12] and observed experimentally [17]. Currently, most works focus on searching for new TI materials [18] and novel transport properties [19–21]. However, the electron states in TI nanostructures, e.g., QDs, remains relatively unexplored.

In this Letter, we consider the quantum dots formed in a HgTe heterostructure with an inverted band structure. We find that the fully spin-polarized quantum states in the gap of the QD show a ringlike density distribution and spin-angular momentum locking. These states arise from the quantization of the edge states along the circumference of the QD, and its energies show an approximately linear dependence on the angular momentum. Importantly, these states are optical dark states that can be used in quantum information storage. A perpendicular magnetic field induces the persistent current and magnetic moment which oscillate with increasing magnetic fields, i.e., the Aharonov-Bohm effect. This effect offers us a possibility for detecting these exotic states by using the SQUID or STM techniques.

We consider a QD formed in a HgTe heterostructure by using the etching technique as shown schematically in Fig. 1 [22]. The low-energy electron states are described by a four-band effective Hamiltonian with a lateral confinement in the basis $|e\uparrow\rangle$, $|hh\uparrow\rangle$, $|e\downarrow\rangle$, and $|hh\downarrow\rangle$ [12]:

$$H_{4\times4} = \begin{bmatrix} H(k) & 0 \\ 0 & H^*(-k) \end{bmatrix}, \tag{1}$$

where $\mathbf{k} = (k_x, k_y)$ is the in-plane momentum of carriers, $H(k) = [\varepsilon(k)]I_{2\times2} + d^i(k)\sigma^i + V(\rho)\sigma^3$, $I_{2\times2}$ is a 2×2 unit matrix, and σ^i $(i = 1, 2, 3)$ are the Pauli matrices. $\varepsilon(k) = C - D(k_x^2 + k_y^2)$, $d^1(k) = Ak_x$, $d^2(k) = Ak_y$, and $d^3(k) = M(k) = M - B(k_x^2 + k_y^2)$. The parameters A, B, C, D, and M depend on the thickness of the HgTe quantum well [12]. Notice that the Hamiltonian is block-diagonal and possesses the time-reversal symmetry for the upper and lower 2×2 blocks. M is an important parameter that can be used to describe the band insulator with a positive

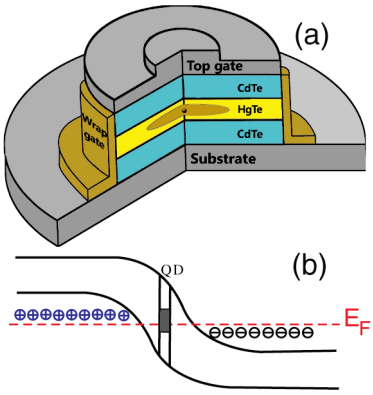

FIG. 1 (color online). (a) Schematic of a quantum dot formed in a HgTe heterostructure using the etching technique. (b) Schematic of electrical injection of electrons and holes into a HgTe QD (the shaded region) embedded in a *p-n* junction.

gap ($M > 0$) and topological insulator with a negative gap ($M < 0$) cases. The confining potential $V(\rho)$ of QD can be simulated by a hard-wall potential: $V(\rho) = 0$, for $\rho < R$, and ∞, otherwise; R is the radius of the hard-wall disk. Other confining potentials, e.g., parabolic confinement, show the essentially same energy spectrum; we omit it here for brevity. The eigenstates and eigenenergies can be obtained numerically by expanding the wave function $\Psi_i = \sum_{n,m} C^{(i)}_{n,m} \varphi_{n,m}$ in terms of the Bessel basis for the hard-wall disk, where the index i corresponds to the different spin projection $S_z = \pm 1/2, \pm 3/2$. $C^{(i)}_{n,m}$ is the expanding coefficient. For a hard-wall disk, the basis function φ_{nm} can be expressed as $\varphi_{nm} = \mathbb{N}_C J_m(k^m_n \rho/R) e^{im\varphi}$, where k^m_n is the nth zero point of the first kind of the cylinder Bessel functions $J_m(x)$, $\mathbb{N}_C = 1/[\sqrt{\pi} R J_{m+1}(k^m_n)]$. $m = 0, \pm 1, \pm 2 \ldots$ is the quantum number of the angular momentum. Because the Hamiltonian has cylindrical rotation symmetry, the total angular momentum along the z direction is in conservation: $[\hat{J}_z, \hat{H}_0] = 0$. Where $\hat{J}_z = \hat{L}_z + \hat{S}_z$, L_z is the orbit azimuthal angular momentum, and $\hat{S}_z$ is the total spin $\hat{S}$ projection onto the z direction. Therefore the total azimuthal angular momentum quantum number j, the eigenvalue of J_z, is a good quantum number. Also we notice that the off-diagonal elements in the Hamiltonian (1) only couple the basis functions with the angular momenta $e^{im\varphi}$ and $e^{i(m+1)\varphi}$. In the presence of an external perpendicular magnetic field, the canonical momentum is $\mathbf{P} = \mathbf{p} + e\mathbf{A}$. $\mathbf{A} = \mathbf{B} \times \mathbf{r}/2$ is the vector potential adopting the symmetric gauge. The number of eigenstates used in the expansion is chosen to ensure the convergence of the calculated energies of the quantum states within and nearby the bulk gap.

For the edge states, we can obtain the analytical expression of the energy and wave function. By using the trial wave function [20] $\psi = e^{\lambda(\rho - R)}(e^{im\varphi}, e^{i(m+1)\varphi})^T$ in the polar coordinate. The variational parameter λ can be given from the secular equations for the upper block of the Hamiltonian (1):

$$[\lambda^2 - (m/R)^2]^2 - (a + b)[\lambda^2 - (m/R)^2] - c = 0, \quad (2)$$

where $a = -2[D(E - C) + BM]/B_+B_-$, $b = A^2/B_+B_-$, $F = (a + b)/2$, and $c = -(M^2 - E^2 - C^2 + 2CE)/B_+B_-$. To obtain the above equation, we take $\rho \approx R$ because the edge states are localized at the boundary of the QD. The variation parameter and the energy can be obtained as $\lambda_{1,2} = \sqrt{(m/R)^2 + F \pm \sqrt{F^2 + (E^2 - M^2 + C^2 - 2CE)/B_+B_-}}$, $E = (BC - DM)/B \pm A\sqrt{1 - (D/B)^2}\, m/R$.

We show the energy spectra of a HgTe QD with a hard-wall confining potential as a function of the angular momentum $m = \langle L_z \rangle$ in Fig. 2 [12]. In Fig. 2, we consider two different cases: the band insulator ($M > 0$) and the topological insulator ($M < 0$) cases. Comparing Fig. 2(a) with Fig. 2(b), one can see that the quantum dot spectrum is gapped for the band insulator QD case ($M > 0$), which is similar with that of the conventional semiconductor QDs. But for the topological insulator QD case ($M < 0$), the new quantum states emerge in the whole energy spectrum, even in the gap. These states show a linear energy dispersion, i.e., the Dirac spectrum, against the angular momentum m in the bulk gap. The energy spectrum of these states [the red and blue squares and circles in Fig. 2(b)] shows symmetric respect to the angular momentum m due to the time-reversal symmetry. In order to understand the physical origin of these states, we plot the density distribution of the quantum states appearing within the bulk gap in Figs. 2(c) and 2(d). Figure 2(c) shows the density distributions of the lowest conduction band electron states, which peak at the center of the QDs as in conventional semiconductor quantum dots. Figure 2(d) describes the density distribution of the new quantum states nearby the Dirac point. Surprisingly, one can see that the state localizes at the edge of the hard-wall QD and shows the ringlike density distribution. We would stress that all these new quantum states carry approximately half-integer angular momentums $m = I \pm 1/2$, where the integer $I = 0, \pm 1, \pm 2, \ldots$ [see the inset in Fig. 2(b)], and show the homocentric ringlike density distributions. We name these exotic quantum states the ringlike edge states (RESs) in this Letter. We calculate the dependence of the energies of the bulk QD states and the RESs on the size of the QD in Fig. 3(a). For the quantum states arising from the quantized electron bulk states localized at the center of the QD, the energy spectrum shows a linear dependence on the inverse of the area of the QD [see the inset in Fig. 3(a)], i.e., $1/R^2$.

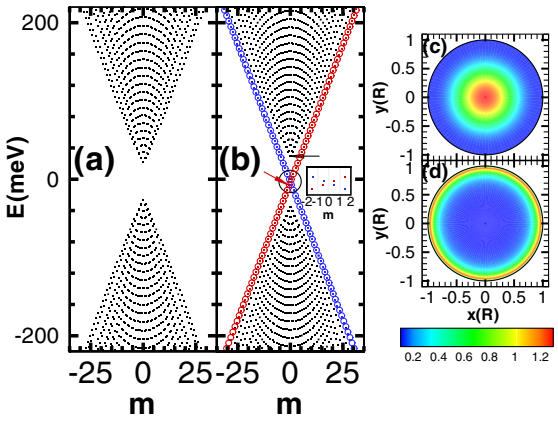

FIG. 2 (color online). Energy spectra of the HgTe QDs in the band insulator ($M > 0$) (a) and topological insulator ($M < 0$) (b) cases as a function of the angular momentum m. The RESs are denoted by the red (rotating clockwise) and blue (rotating counterclockwise) squares. The red and blue circles are plotted from the analytical solutions. The inset is the enlarged circle region near the Dirac point. (c) The density distributions of the lowest conduction band electron states [marked by the black arrow in (b)] in the QD; (d) the same as (c), but for the RES [marked by the red arrow in (b)] near the Dirac point. The QD radius $R = 55$ nm, and $M = -30$ meV.

Interestingly, the energies of the RESs display a linear dependence on the inverse of the circumference of the QD, i.e., $1/R$. This feature indicates clearly that these exotic quantum states come from the quantization of the edge states in two-dimensional topological insulators along the circumference of the hard-wall disk. The RESs are equally spaced in the energy spectrum [see Fig. 2(b)] because of the new quantization rule $m = I \pm 1/2$ and show the linear energy dispersion against the angular momentum m. This characteristic means that electrons in the RESs behave like massless Dirac fermions. When this massless Dirac fermion is confined in a disk, its lowest energy modes should be the whispering gallery mode, similar to a photon confined in a cylinder cavity. This gives us an intuitive picture to understand the origin of these exotic ringlike quantum states in QDs. From Fig. 3(b), one can see that the energy level spacing $\Delta E = E_m - E_{m-1}$ of the RESs (the gap of the bulk states $E_g = E^c_{m=0} - E^v_{m=0}$, where the indices c and v denote the conduction and valence bands, respectively) in the QD increase linearly as the inverse of the radius $1/R$ (area $1/R^2$) of the QD increases. The slight difference between the numerical and analytical results arises from the approximation $\rho \approx R$ adopted in our derivation.

Interestingly, these ringlike states are fully spin-polarized and show a spin-angular momentum locking. In Fig. 3(c), there are two kinds of these ringlike quantum states in which spin-up electrons rotate clockwise and spin-down electrons rotate counterclockwise [see Fig. 3(c)]. This opposite spin orientation is the consequence of the time-reversal symmetry in the four-band Hamiltonian (1). Note that the spin projection of edge states $\langle S_z \rangle$ is not a good quantum number and varies significantly with increasing the angular moment m. For the edge states rotating clockwise (the spin-up branch) and counterclockwise (the spin-down branch), the spin orientation $\langle S_z \rangle$ varies approximately from 0.6 to 1.4 (-0.6 to -1.4), which indicates that the mixing between the electron and the hole states changes with the angular momentum and therefore destroys the spin conservation. The spin orientation $\langle S_z \rangle$ is symmetric with respect to the angular momentum $\langle m \rangle$, i.e., rotating clockwise and counterclockwise. Interestingly, this degeneracy $E_m = E_{-m}$ is lifted by a weak magnetic field; thus, one can get a fully spin-polarized electron state by controlling the number of electrons in such a QD at low temperatures.

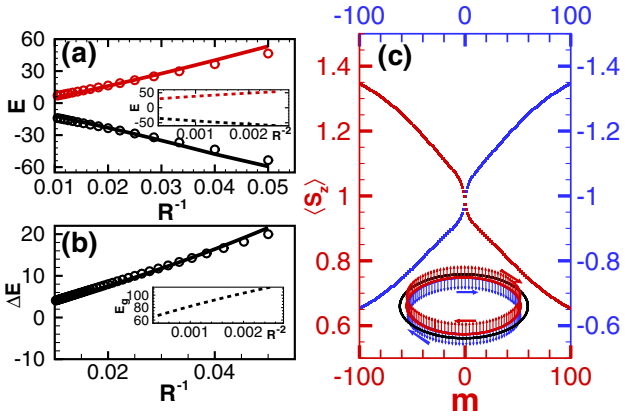

FIG. 3 (color online). (a) The energies of the up (red line) and down (black line) branches of the RESs vs the inverse of the radius of the QD $1/R$. The inset shows the dependence of the energies of the electron states in the bulk conduction (red dashed line) and valence (black dashed line) bands on the inverse square of the radius of the QD $1/R^2$, respectively. (b) The energy level spacing ΔE of the RESs vs the $1/R$; the inset shows the bulk energy gap of the QD vs $1/R^2$. The circles in (a) and (b) are obtained from the analytical expression of the edge states. (c) The spin projection $\langle S_z \rangle$ for the ringlike edge states with the different angular momentum m. The inset is the schematic of the spin orientation of the RESs in the QD. $R = 55$ nm, and $M = -30$ meV.

Next we turn to discuss the optical property of these edge states in QDs. The absorption spectra of the QD $\alpha(\hbar\omega) = \frac{\pi e^2}{m_0^2 \epsilon_0 c n \omega V} \sum_{i,f} |\vec{\varepsilon} \cdot P_{if}|^2 \delta(E_f - E_i - \hbar\omega)$, where n is the refractive index, c is the speed of light in vacuum, ϵ_0 is the permittivity of vacuum, m_0 is the free-electron mass, and $\vec{\varepsilon}$ is the polarization vector of the incident light. We are interested only in the vertical optical transition between the up and down branches of the edge states near the Dirac point, i.e., within the bulk gap. The momentum matrix $\mathbf{P} \propto \partial H_{4\times4}/\partial \mathbf{k}$ is block-diagonal and will not couple the up and down branches of the edge states belonging to the spin-up and spin-down families; therefore, the vertical circular transition between the up and down branches is forbidden because of the conservation of the angular moment. It means that these RESs are optically inactive within the electric dipole approximation, i.e., the dark states. However, the RESs also provide us a possibility to store quantum information in these dark states, e.g., an electron-hole pair in the RESs formed by electric injection [see Fig. 1(b)].

Finally, we study the effect of the magnetic field on these RESs. We consider an external magnetic field applied perpendicularly to a HgTe QD plane. Figure 4(a) shows the magnetic levels in a HgTe QD ($M < 0$) including the bulk and edge states. The energy spectra display many crossing points in the bulk gap region. This is because the spectrum of the RESs is similar to that of a quantum ring. The energy spectra become no longer symmetric with respect to the angular moment $\langle m \rangle$ because the magnetic field breaks the time-reversal symmetry [see Fig. 4(b)]. The Dirac point is shifted left, and the edge states rotating clockwise (counterclockwise) are strongly squeezed (separated), since the Lorentz force induced by the magnetic field suppresses (enhances) the electron rotating clockwise (counterclockwise). At a high magnetic field ($R \gg l_B$), the edge states rotating clockwise are pushed into the bulk states and cannot be seen in the spectra as shown in Fig. 4(b).

It is well known that a magnetic field can induce a persistent current in mesoscopic rings and even type-II

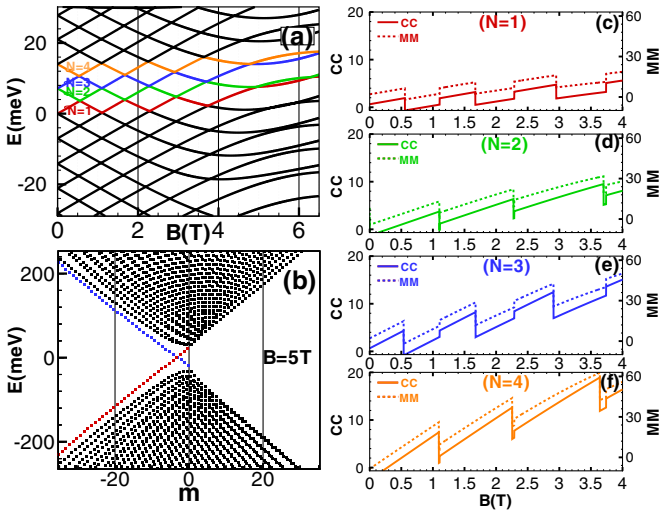

FIG. 4 (color online). (a) The magnetic level fan in a HgTe QD with an inverted band structure. (b) The energy spectrum in the presence of magnetic fields for the TI QD. (c)–(f) The persistent charge current (CC) (solid line) and magnetic moment (MM) (dashed line) in a TI QD against the magnetic fields for a different electron number N. The persistent CC is in units of $2NE_0/\Phi_0$ ($2N * 2nA$ for the hard-wall disk), where $E_0 = \hbar^2/[2m^*(R)^2]$. $R = 55$ nm, and $M = -30$ meV. The magnetic moment is in units of $N\mu_B$, where $\mu_B = e\hbar/(2m_e)$. The red, green, blue, and orange curves indicate different electrons $N = 1$, 2, 3, and 4 filled in the edge states [see (a)].

quantum dots, i.e., the Aharonov-Bohm effect [23–25], which oscillates with increasing magnetic fields. Such a quantum mechanical phenomenon is never observed in type-I QD systems. Interestingly, this phenomenon can be found in this topological insulator QD system, because the unique density distributions of the RESs show a ringlike behavior and are almost localized at the boundary of the hard-wall disk. The persistent current for a single TI QD can be obtained by $I = \int \hat{j}_c(r)d\vec{r}$, where the current density operator $\hat{j}_c(r) = [\hat{\rho}\,\hat{v} + \hat{v}\,\hat{\rho}]/2$, and the magnetic moment $\vec{M}$ generated by the persistent current is given by $\vec{M} = \int \vec{r} \times \hat{j}_c(r)d\vec{r}/2$, where $\hat{\rho}$ is the electron density operator and $\hat{v}$ is the electron group velocity operator along the tangential direction. From Figs. 4(c)–4(f), one can see that the magnitude of the magnetic moment induced by the persistent current depends on the electron numbers in the QD and ranges from 20 to $200\mu_B$, which is beyond the limit of resolution and sensitivity of near-field SQUID magnetometry (around $1–10\mu_B$) [26]. The persistent charge current and the magnetic moment are periodic functions of magnetic fields, exhibiting many linear segments with a fixed slope ratio. The periodicity of the persistent charge current for a different electron number N is almost the same. This feature can be understood from the crossing points in the magnetic energy level spectrum in Fig. 4(a). When the magnetic field sweeps across the points, the persistent current and magnetic moment oscillate. The oscillation of the magnetic moment provides us a possibility to detect these exotic quantum states in HgTe QDs by using the near-field SQUID technique at a low temperature [26,27].

In summary, we study the exotic quantum states in quantum dots formed in a HgTe heterostructure with inverted band structures. The RESs appear in the bulk gap of the QDs, show ringlike density distributions, and are optically inactive. This feature is in sharp contrast to that of the conventional semiconductor quantum dots with normal band structures. The oscillating persistent currents and magnetic moments can be found as the perpendicular magnetic fields increase, which make it possible to detect these quantum states by utilizing the nano-SQUID technique.

This work was partly supported by the NSFC Grants No. 60525405 and No. 10874175.

[1] D. Loss and D. P. DiVincenzo, Phys. Rev. A **57**, 120 (1998); A. Imamoglu *et al.*, Phys. Rev. Lett. **83**, 4204 (1999).
[2] R. Hanson *et al.*, Rev. Mod. Phys. **79**, 1217 (2007).
[3] M. A. Kastner, Rev. Mod. Phys. **64**, 849 (1992).
[4] N.-M. Park *et al.*, Phys. Rev. Lett. **86**, 1355 (2001).
[5] S. Fafard *et al.*, Science **274**, 1350 (1996).
[6] A. Martí *et al.*, Phys. Rev. Lett. **97**, 247701 (2006).
[7] M. Grundmann *et al.*, Phys. Rev. Lett. **74**, 4043 (1995).
[8] T. Hayashi *et al.*, Phys. Rev. Lett. **91**, 226804 (2003).
[9] L. P. Kouwenhoven *et al.*, Science **278**, 1788 (1997).
[10] X. C. Zhang *et al.*, Phys. Rev. B **63**, 245305 (2001).
[11] C. L. Kane and E. J. Mele, Phys. Rev. Lett. **95**, 226801 (2005); **95**, 146802 (2005).
[12] B. A. Bernevig, T. L. Hughes, and S. C. Zhang, Science **314**, 1757 (2006).
[13] L. Fu and C. L. Kane, Phys. Rev. B **76**, 045302 (2007); J. C. Y. Teo, L. Fu, and C. L. Kane*ibid.* **78**, 045426 (2008).
[14] X. L. Qi, T. L. Hughes, and S. C. Zhang, Phys. Rev. B **78**, 195424 (2008).
[15] X. L. Qi and S. C. Zhang, Phys. Today **63**, No. 1, 33 (2010).
[16] M. Z. Hasan and C. L. Kane, Rev. Mod. Phys. **82**, 3045 (2010).
[17] M. König *et al.*, Science **318**, 766 (2007).
[18] H. J. Zhang *et al.*, Nature Phys. **5**, 438 (2009); D. Hsieh *et al.*, Nature (London) **452**, 970 (2008); H. Lin *et al.*, Phys. Rev. Lett. **105**, 036404 (2010).
[19] D. Hsieh *et al.*, Nature (London) **460**, 1101 (2009).
[20] B. Zhou *et al.*, Phys. Rev. Lett. **101**, 246807 (2008).
[21] E. B. Sonin, Phys. Rev. B **82**, 113307 (2010).
[22] J. Hinz *et al.*, Semicond. Sci. Technol. **21**, 501 (2006).
[23] I. R. Sellers *et al.*, Phys. Rev. Lett. **100**, 136405 (2008).
[24] J. H. Bardarson, P. W. Brouwer, and J. E. Moore, Phys. Rev. Lett. **105**, 156803 (2010).
[25] Y. Zhang and A. Vishwanath, Phys. Rev. Lett. **105**, 206601 (2010).
[26] V. Bouchiat, Supercond. Sci. Technol. **22**, 064002 (2009).
[27] W. Rabaud *et al.*, Phys. Rev. Lett. **86**, 3124 (2001).